Atmos. Chem. Phys. Discuss., 15, 21415–21448, 2015
www.atmos-chem-phys-discuss.net/15/21415/2015/
doi:10.5194/acpd-15-21415-2015

Atmospheric Chemistry and Physics Discussions

Identification of particulate organosulfates in three megacities at the middle and lower reaches of the Yangtze River

X. K. Wang[1,2,a], S. Rossignol[3,a], Y. Ma[1,2], L. Yao[1,2], M. Y. Wang[1,2], J. M. Chen[1,2], C. George[3], and L. Wang[1,2]

[1]Shanghai Key Laboratory of Atmospheric Particle Pollution and Prevention (LAP[3]), Department of Environmental Science & Engineering, Fudan University, Shanghai 200433, China
[2]Fudan Tyndall Centre, Fudan University, Shanghai 200433, China
[3]Université de Lyon 1, Lyon, 69626, France; CNRS, UMR5256, IRCELYON, Institut de Recherches Sur la Catalyse et l'Environnement de Lyon, Villeurbanne, 69626, France
[a]These authors contributed equally to this work.

Received: 28 May 2015 – Accepted: 19 July 2015 – Published: 10 August 2015

Correspondence to: C. George (christian.george@ircelyon.univ-lyon1.fr) and L. Wang (lin_wang@fudan.edu.cn)

Published by Copernicus Publications on behalf of the European Geosciences Union.

ACPD
15, 21415–21448, 2015

Abstract

$PM_{2.5}$ filter samples have been collected in three megacities i.e., Wuhan (WH), Nanjing (NJ), and Shanghai (SH) at the middle and lower reaches of the Yangtze River, respectively. Analysis of those samples using an ultra-high performance liquid chromatography (UHPLC) coupled to an orbitrap mass spectrometer (MS) allowed detection of about two hundred particulate organosulfates (OSs), including dozens of nitrooxy-organosulfates, at each location. While aliphatic OSs represented more than 78 % of the detected OSs at the three locations, aromatic OSs were much less abundant. OSs with two to four isomers accounted for about 50 % of the total OSs on average in these megacities, and the percentage of OSs with six and more isomers in WH was more significant than those in SH and NJ. The average molecular weight, and the degrees of oxidation and saturation of OSs in the WH summer samples were greater than those in WH winter samples. In SH, the average molecular weight and the degree of oxidation of OSs in summer samples were greater than those in winter samples, but the degree of saturation was similar between the two seasons. In summer, the average molecular weight, and the degrees of oxidation and unsaturation of OSs were smallest in WH among the three cities. Between NJ and SH, the average molecular weight and the degree of saturation of OSs were close and the degree of oxidation of OSs in NJ was smaller. Kendrick mass defect diagrams and Van Krevelen diagrams indicated that the characteristics of identified OSs between in NJ and in SH shared better similarity. In addition, the identity and abundance of OSs in SH showed clear seasonal and diurnal variations. OSs in summer were more abundant than they were in winter due to stronger photochemical reactions in summer. The relative abundance of OSs at night was greater than that in the daytime and more nitrooxy-OSs existed at night, probably because of active NO_3 radical chemistry at night. In SH summer samples, OSs with 5 and 10 carbons (C_5 and C_{10}) were the most abundant, indicating the importance of isoprene and monoterpenes as precursors of OSs, whereas the relative abundances

ACPD
15, 21415–21448, 2015

of OSs with 8, 9, and more than 14 carbons (C_8, C_9, and C_{14+}) were also high in SH winter samples, urging the need to further understand the precursors of OSs.

1 Introduction

Atmospheric aerosols can scatter and absorb sunlight, provide cloud condensation nuclei, and hence have significant impacts on the air quality and the climate (Andreae and Crutzen, 1997; Hallquist et al., 2009). Aerosol particles contain a large fraction of toxic chemical substances and are harmful to the human health (Lee et al., 2013). Organosulfates (OSs), i.e., sulfate esters and their derivatives formed from atmospheric heterogeneous and multiphase chemical reactions (Ma et al., 2012), are a class of organic components that contribute to the total abundance of atmospheric aerosol particles (Tolocka and Turpin, 2012).

Recent years have seen tremendous progresses of our understanding on the formation mechanisms of OSs, while uncertainties well remain. Existing experimental studies show that isoprene-derived epoxide (IEPOX) and methacrylic acid epoxide (MAE) are formed during oxidation of isoprene under low- and high-NO_x conditions, respectively. Subsequent acid catalyzed-reactions of IEPOX and MAE in the presence of sulfates can lead to the formation of OSs (Darer et al., 2011; Surratt et al., 2010; Paulot et al., 2009). OSs can be formed from reactions between α-pinene and OH radical, NO_3 radical, and O_3 in the presence of sulfates, from β-pinene under high-NO_x conditions, from ozonolysis and photochemical reactions of other monoterpenes i.e., α-terpinene and γ-terpinene, and from sesquiterpene i.e., β-caryophyllene under acidic conditions (Surratt et al., 2008; Iinuma et al., 2007a, b; Chan et al., 2011). In addition, both reactive uptake of carbonyl compounds on sulfuric acid or sulfates (Liggio et al., 2005) and the hydrolysis reactions of organonitrates can lead to formation of OSs (Darer et al., 2011; Hu et al., 2011).

Identification and quantification of OSs in atmospheric particulate samples have been widely performed around the world (e.g., Kristensen and Glasius, 2011; Stone

ACPD
15, 21415–21448, 2015

et al., 2009; Olson et al., 2011; Zhang et al., 2012). Surratt et al. identified, for the first time, isoprene- and α-pinene-derived OSs in ambient aerosols in the US southeast area using high performance liquid chromatography coupled to electrospray mass spectrometry (Surratt et al., 2007). Many studies indicate that the total abundance of OSs varies from one region to another. OSs accounted for about 4 % of the total organic mass in ambient aerosols over the southeast Pacific Ocean (Hawkins et al., 2010), whereas this contribution was estimated to about 30 % at the forested site of K-puszta in Hungary during a summer campaign (Surratt et al., 2008). The abundance of a given OS also shows clear variation between different sampling locations. Four aromatic OSs estimated to be 234.4 pg m^{-3} in atmospheric $PM_{2.5}$ in Pakistan, were for example much less abundant in California, US (8.9 pg m^{-3}) or Nepal (3.9 pg m^{-3}) (Staudt et al., 2014). At a given location, seasonal variations of OSs exist. Ma et al. (2014) showed that the total mass concentration of seventeen OSs were the highest in summer and the lowest in winter, while no clear seasonal trend in the mass concentration of benzyl sulfate (BS) was observed. However, BS showed the highest concentration in winter and the lowest one in summer in Lahore, Pakistan (Kundu et al., 2013), which underlies the role of both regional constraints and meteorological conditions.

Recently, ultra-high resolution mass spectrometer has been applied to the identification of OSs in atmospheric aerosols samples. Owing to the high mass resolution and high mass accuracy of the ultra-high resolution mass spectrometer, molecular formulas of analytes can be tentatively determined without authentic standards as required with a low resolution mass spectrometer. The studies of Lin et al. (2012a, b), performed on aerosols sampled at a rural location of the Pearl River Delta Region in China, suggests that the arbitrary signal intensities of OSs obtained from the humic-like fraction are often the strongest in the electrospray ionization ultra-high resolution mass spectra, and that the degrees of oxidation of OSs and nitrooxy-OSs are quite high. Using a similar approach, O'Brien et al. (2014) showed that a significant portion of OSs was formed from biogenic precursors through the epoxide pathway in Bakersfield, CA, USA. In addition, by using a mixture of acetonitrile and toluene instead of a mixture of acetonitrile

ACPD
15, 21415–21448, 2015

and water as the working solvent for nano-DESI ionization, Tao et al. (2014) identified many OSs with long aliphatic carbon chains and low degrees of oxidation and unsaturation, presumably formed from precursors emitted by cars, in Shanghai (SH) aerosol samples, and OSs formed from biogenic precursors, in contrast, in Los Angeles.

Although it has been accepted that OSs are an important component of ambient particulate matters, studies on the characteristics of ambient OSs are rather sparse in China, especially in the Yangtze River region. Ma et al. (2014) identified and quantified seventeen OSs in SH. Tao et al. (2014) compared characteristics of OSs, such as the degrees of oxidation and saturation, between samples from SH and Los Angeles. While SH has been a relative hotspot for OSs identification, the characteristics of OSs in the general Yangtze River region are yet to be elucidated. Wuhan (WH), Nanjing (NJ) and SH are three megacities at the middle and lower reaches of the Yangtze River, respectively. Tremendous amounts of energy are consumed owing to the large population and rapid economic development, leading to extensive emissions of anthropogenic pollutants including particulate matters, volatile organic compounds (VOCs), sulfur dioxide, and nitrogen oxides (Huang et al., 2011; Wang et al., 2013). At the same time, these three cities are located in the subtropical zone with high emissions of biogenic VOCs (Guenther et al., 1995). Hence, substantial amounts of OSs are likely to exist in WH, NJ, and SH aerosol particles. In this study, OSs were specifically searched for in WH, NJ, and SH $PM_{2.5}$ samples using an UHPLC coupled to an Orbitrap-MS. Characteristics of OSs including the number of isomers, molecular weight, the degrees of oxidation and unsaturation, and seasonal and diurnal variations are analyzed and compared. Their potential precursors in those megacities are also discussed.

ACPD
15, 21415–21448, 2015

2 Material and methods

2.1 Collection of $PM_{2.5}$ samples

Eight $PM_{2.5}$ samples were collected at three locations i.e., two at WH, two at NJ, and four at SH, as shown in Fig. 1 and Table 1. Daily samples at WH were collected during 26–27 January 2012 and 15–16 June 2012, respectively. The WH site was located on the rooftop of a dormitory building that is about 20 m above ground at ZhongNan University of Economics and Law (30°29′ N, 114°24′ E) near a commercial street with light traffic. NJ samples were collected during 29–30 August 2012, and each sample for 12 h. The NJ site was located in the Chinese national meteorology observatory facility at the Nanjing University of Information Science and Technology (32°12′ N, 118°42′ E), which is about 15 km to the north of the downtown area and about 2 km to the west of clusters of steel mills and petrochemical refinery facilities (Zheng et al., 2015). SH samples were collected during 17–18 January 2013 and 28–29 July 2013, respectively, and each sample for 12 h. The SH site was located on the rooftop of a teaching building at Fudan University (31°18′ N, 121°30′ E), which is about 20 m above ground with surrounding residential and commercial properties and a major highway to the south of the site (Xiao et al., 2015; Ma et al., 2014).

$PM_{2.5}$ was collected onto quartz filters (Φ90 mm, Whatman Company, UK) using a middle-flow impact aerosol sampler (Qingdao Hengyuan Tech Co., Ltd., HY-100) operating at 100 lpm. All filters were prebaked at 500 °C for 5 h to remove residual organics before usage. After sample collection, filters were wrapped in a prebaked aluminum foil and stored at −20 °C before further analysis.

2.2 Samples analysis

One-fourth of each filter was put into an amber vial with 6 mL of methanol (Optima® LC/MS, Ficher Scientific, UK) and shaken for 20 min on an orbital shaker set at 1000 rpm. The extract was then filtered through a glass syringe onto a 0.2 µm PTFE

ACPD
15, 21415–21448, 2015

membrane (13 mm, Pall Corporation, USA). These two steps were performed twice and the extracts of each filter were recombined and blown to almost dryness under a gentle stream of nitrogen. The extracts were reconstituted in 1 mL of a 1 : 1 v/v mixture of water (Optima® LC/MS, Ficher Scientific, USA) and acetonitrile (Optima® LC/MS, Ficher Scientific, USA). Blank filters were processed and analyzed in an identical way, and blank correction has been made accordingly. For the analysis, 100 µL of the final reconstituted extract was diluted by a factor 2 adding 100 µL of water. 5 µL of these diluted solution (50 µL in the case of the NJ daytime sample) were analyzed by an ultra-high performance liquid chromatograph (UHPLC, Dionex 3000, Thermo Scientific, USA) coupled to a Q-Exactive Hybride Quadrupole-Orbitrap MS (Thermo scientific, USA) in the mass range of m/z 50–750 Th. The efficiency and the repeatability on three replicates of the extraction protocol were checked on four standards, methyl sulfate, octyl sulfate, dodecyl sulfate and camphor sulfonic acid. Protocol and results are given in the Supplement.

Analytes were separated using a Waters Acquity HSS T3 column (1.8 µm, 100 mm × 2.1 mm) with mobile phases consisting of (A) 0.1 % formic acid in water (Optima® LC/MS, Ficher Scientific, USA) and (B) 0.1 % formic acid in acetonitrile (Optima® LC/MS, Ficher Scientific, USA). The concentration of eluent B was initially kept at 1 % for 2 min, then increased to 100 % in 11 min, kept at 100 % for 2 min, then decreased to 1 % in 0.1 min, and kept at 1 % for 6.9 min. The Q-Exactive Hybride Quadrupole-Orbitrap mass spectrometer is equipped with a heated electrospray ionization source. It was operated in the negative ion mode with a spray voltage of −3.0 kV and a mass resolving power of 140 000 at m/z 200 amu.

2.3 Data processing

The obtained chromatograms were analyzed with a Progenesis QI software (V1.0, Waters Corporation) by assuming that the extracted ions in the m/z range of 50–750 amu were $[M\text{-}H]^-$ formed from loss of a proton from the analytes. The LC separation al-

ACPD
15, 21415–21448, 2015

lowed identifying this pseudo-molecular ion and potential in-source formed adducts for a same chromatographic peak. A molecular formula calculator was used to assign all mathematically possible formulas for the extracted ions with a mass tolerance of ±2 ppm. The obtained molecular formula can be expressed as $C_cH_hO_oN_nS_s$, where c is the number of carbon atoms confined in the range of 1–40, h is the number of hydrogen atoms confined in the range of 2–80, o is the number of oxygen atoms confined in the range of 0–40, n is the number of nitrogen atoms confined in the range of 0–3, and s is the number of sulfur atoms confined in the range of 0–2. Formulas were further constrained by setting H/C, O/C, N/C, S/C, and DBE (Double Bond Equivalent) / C ratios in the range of 0.3–3.0, 0–3, 0–0.5, 0–0.2, and 0–1, respectively, to assure that the obtained compound exists in nature (Fuller et al., 2012; Wozniak et al., 2008). Compounds that satisfy the above criteria and present a number of oxygen atoms greater than $4s + 3n (4s + 3n \leq o)$ were tentatively regarded as OSs or nitrooxy-OSs. In this study, the abundance of an OS refers to the area of its chromatographic peak, and the number of isomers for an OS is based on the number of the chromatographic peaks with the same m/z values (one characteristic chromatogram is shown in Fig. S1 in the Supplement). Then the arbitrary abundances of all isomers for a formula are added up. The arbitrary abundance of the most abundant OS or nitrooxy-OS in each sample is defined as 100 %, and only OSs and nitrooxy-OSs with an arbitrary abundance larger than 0.5 % of the most abundant one in the same sample are presented. The signals to noise ratios of the least abundant OSs in each sample are far greater than 10. Note that the arbitrary abundance of an OS does not reflect the true relative concentration because the ionization efficiency of OSs vary a lot in electrospray ionization depending on molecular structures and sample matrix.

The DBE value of a molecule reflects the degree of its unsaturation. The DBE value can normally be calculated by Eq. (1).

$$\mathrm{DBE} = \frac{2c + 2 + n - h}{2} \quad (1)$$

ACPD
15, 21415–21448, 2015

Not taking into account the two double bonds involved in each sulfate group, the DBE values of OSs calculated by Eq. (1) represent the unsaturation degree of the side carbon chain (eventually bearing oxygen and nitrogen atoms). However, it is important to note that this equation adds one DBE unit for each nitrate group. Molecular formulas with DBE < 0 and formulas that disobey the nitrogen rule were discarded. The difference between the DBE value and the number of N atoms (DBE-n), is the most conservative criterion to determine whether a compound is aliphatic: the number of OSs with (DBE – n) < 4 can be regarded as the minimum number of aliphatic OSs (Lin et al., 2012b).

Both DBE/C and Aromaticity index (AI) could be used as criterions to determine whether a compound contains aromatic rings, with a threshold of DBE/C > 0.67 and AI > 0.5, respectively, but AI is more conservative (Koch and Dittmar, 2006). The value of AI can be calculated according to Eq. (2).

$$\mathrm{AI} = \frac{\mathrm{DBE_{AI}}}{\mathrm{C_{AI}}} = \frac{1 + c - o - s - (0.5\,\mathrm{h})}{c - o - s - n} \quad (2)$$

where $\mathrm{DBE_{AI}}$ represents the sum of the minimum number of C=C double bonds and the number of rings in a formula containing heteroatoms, and $\mathrm{C_{AI}}$ represents the difference between the number of carbon and the number of potential double bonds caused by heteroatoms. If $\mathrm{DBE_{AI}} \le 0$ or $\mathrm{C_{AI}} \le 0$, then AI is defined to be zero. In contrast, AI > 0.5 and AI ≥ 0.67 indicate the existence of aromatic and fused aromatic ring structures in a compound, respectively (Koch and Dittmar, 2006).

In the Kendrick mass defect diagram (KMD diagram), $\mathrm{CH_2}$ (14.00000) was chosen as a base unit. The Kendrick mass ($\mathrm{KM_{CH_2}}$) and the Kendrick mass defect ($\mathrm{KMD_{CH_2}}$) can be determined by Eqs. (3) and (4), respectively.

$$\mathrm{KM_{CH_2}} = \text{Observed Mass} \times \left(\frac{14.00000}{14.01565}\right) \quad (3)$$

$$\mathrm{KMD_{CH_2}} = \text{Nominal Mass} - \mathrm{KM_{CH_2}} \quad (4)$$

ACPD
15, 21415–21448, 2015

where Observed Mass is the mass measured by the mass spectrometer, and Nominal Mass is the rounded integer mass of a compound.

3 Results and discussion

3.1 General characteristics of OSs

Table 1 summarizes the sampling time and locations of the eight samples and the average characteristics of OSs and nitrooxy-OSs detected in each sample. In addition to daily data of WH, daytime and nighttime data of NJ, and daytime and nighttime data of SH, are combined respectively to provide comparable daily data. In Table 1, OSs are categorized into two groups, CHOS (OSs without nitrate substituents) and CHONS (nitrooxy-OSs), according to whether the molecule contains a nitrogen atom and fulfill the $4s + 3n \leq o$ rule or not. More than one hundred formulas of CHOS and dozens of formulas of CHONS have been tentatively identified in each sample.

The mass spectra of identified OSs in summer samples at the three megacities have been reconstructed to present the general characteristics of OSs. In Fig. 2, the x axis corresponds to the molecular weight of identified OSs, the y axis represents the arbitrary abundances, and the number of isomers for an OS is color-coded. Note that the daily WH sample, the NJ nighttime sample, and the combined daily data in SH are presented in Fig. 2, because the amount of the NJ daytime sample analyzed by UHPLC-Orbitrap MS was different from others.

Comparison of the reconstructed mass spectra suggests that the number of OSs with an identical formula and the same number of isomers that could be observed in all three megacities accounted for only 17.6 % of the molecular formulas of identified OSs. Between WH and NJ, the number of OSs with an identical formula accounted for 50.3 % of the molecular formulas of identified OSs, but only 27.9 % also possessed the same number of isomers. Between NJ and SH, the number of OSs with an identical formula accounted for 62.8 % of the molecular formulas of identified OSs, but only 39.4 % also

ACPD
15, 21415–21448, 2015

possessed the same number of isomers. Between WH and SH, the number of OSs with an identical formula accounted for 51.5 % of the molecular formulas of identified OSs, but only 32.3 % also possessed the same number of isomers. Therefore, the number of isomers for an OS in NJ and SH showed greater similarity. This observation is in agreement with the proximity of the two cities compared to the more distant city of WH.

In all three megacities, OSs with two to four isomers accounted for about 50 % of the total OSs. OSs with more than six isomers accounted for the largest proportion and OSs with one isomer were insignificant in WH. In contrast, OSs with more than six isomers were much less and OSs with one isomer represented a substantial proportion in NJ and SH. The distribution of the number of isomers for OSs is one of the main disparities between the WH sample and others.

The gaseous precursors of many OSs in Fig. 2 can be tentatively designated since identical formulas of OSs have been observed from chamber studies. In Fig. 2, OSs with strong arbitrary signal intensities have been labeled with a letter: A, $C_5H_8O_3SO_4$; B, $C_5H_{12}O_3SO_4$; C, $C_6H_{10}O_3SO_4$; D, $C_7H_{12}O_3SO_4$; E, $C_9H_{18}O_2SO_4$; F, $C_5H_{11}O_2NO_3SO_4$; G, $C_9H_{16}O_3SO_4$; H, $C_{10}H_{17}NO_3SO_4$; I, $C_5H_{10}O_1(NO_3)_2SO_4$; J, $C_{16}H_{32}O_2SO_4$; and K, $C_{15}H_{25}NO_3SO_4$. Among these OSs, A, C, D, and G are a series of homologues, and so are E and J. A, B, C, F and I could be derived from isoprene, whereas D and G could be derived from limonene, K from caryophyllene and H from various monoterpenes (i.e. α-pinene, β-pinene, α-terpinene and terpinolene; Chan et al., 2011; Surratt et al., 2008; Gomez-Gonzalez et al., 2008). E and J were characterized by high molecular weights and degrees of saturation, presumably being long-chain aliphatic OSs. In general, many abundant OSs could derive from isoprene, monoterpenes, and sesquiterpenes in summer in three megacities. The relative abundance of J was the highest in WH but much lower relative abundance in NJ and SH. H was the highest in the SH daily spectrum while I was the most abundant in the NJ nighttime sample. I doubtless bears two nitrate groups (two nitrogen atoms in its formula that fulfills the $4s + 3n \leq o$ rule) and is the most abundant in the NJ nighttime sample likely due to active NO_3 radical chemistry at night. F and K, that bear one nitrate group, were

ACPD
15, 21415–21448, 2015

also quite abundant in the NJ nighttime sample, underlying the role of NO_3 chemistry at night.

3.2 Spatio-temporal characteristics of OSs

Table 1 further presents, in addition to the spatio-temporal variations of the number of isomers for an OS and of the abundance of OSs analyzed in the previous session, the spatio-temporal characteristics of OSs in the three megacities by tabulating the average molecular weight, DBE, and elemental ratios of identified CHOS and CHONS. In addition, $(o-3s)/c$ (Tao et al., 2014) and $(o-3s-2n)/c$ have been calculated to illustrate the number of oxygen-containing functional groups per carbon atom for CHOS and CHONS, respectively. These two values derive from the fact that the sulfate and nitrate groups contain respectively three and two more oxygen atoms than do common oxygen-containing groups such as a hydroxyl or a carbonyl moiety. $(o-3s)/c$ and $(o-3s-2n)/c$ can be regarded as a measure of the degree of oxidation of CHOSs and CHONS, respectively.

In Table 1, our data indicate that the average molecular weight and the degrees of oxidation and saturation of OSs in WH summer samples were greater than those in winter samples. In SH, the average molecular weight and the degree of oxidation of OSs in summer samples were greater than those in winter samples, but the degree of saturation was similar between the two seasons. The seasonal variations in average molecular weight and the degrees of oxidation and saturation of OSs are likely due to different precursors between the seasons, and weaker photochemical reactions in winter.

In all the samples, the average molecular weight and the DBE value of CHONS species were generally larger than those of CHOS, because CHONS contains one or two more nitrate groups (the presence of one nitrate group adding one DBE unit). Measuring the O/C ratio of OSs in Bakersfield, CA, USA, O'Brien et al. (2014) indicated that the degree of oxidation of CHONS was larger than CHOS all along the day. A similar trend have been observed for $CHONS_1$ and $CHOS_1$ in SH and Los Angeles aerosol

ACPD
15, 21415–21448, 2015

samples, using $(o-3)/c$ as the measure of the degrees of oxidation (Tao et al., 2014). In our study, however, the average degree of oxidation of CHONS was similarly larger than that of CHOS in the daytime, but smaller at night. The use of the more relevant $(o-3s)/c$ and $(o-3s-2n)/c$ ratios to evaluate the degrees of oxidation of the CHOS and CHONS carbon chain, respectively, allows the direct comparison of the oxidation states of these two groups of compounds and probably explains the fact that we are able to discern such fine variations. Nevertheless, so closed values of oxidation states for OSs and nitrooxy-OSs on a same sample (0.01 to 0.14 units of difference) suggest that the presence of sulfate and/or nitrate groups is not determinant.

The similarity and dissimilarity of OSs in summer between the three megacities can be obtained by comparing the combined daily data in SH and NJ, and the daily sample in WH. The average molecular weight and degree of oxidation of CHONS were the greatest in SH and the lowest in WH, and the degrees of saturation of CHONS in three megacities were similar. On the other hand, the average molecular weight of CHOS in NJ was larger than that in SH. In general, in summer, the average molecular weight, and the degrees of oxidation and unsaturation of OSs were smallest in WH among the three cities. Between NJ and SH, the average molecular weight and the degree of saturation of OSs were close and the degree of oxidation of OSs in NJ was smaller.

The OSs with $(\mathrm{DBE}-n)<4$ accounted for 86.2, 78.5 and 78.3 % of total OSs in summer in WH, NJ, and SH, respectively, suggesting the identified OSs were mainly aliphatic OSs. The number of OSs with $(\mathrm{DBE}-n)\geq 4$ can then be regarded as the maximum number of aromatic OSs. This latter value being slightly higher for SH and NJ, it could indicate a slightly more significant anthropogenic influence in these two cities. The number of OSs with $\mathrm{DBE/C}>0.67$ accounted for 2.2, 5.2 and 7.1 % of total OSs and their abundance accounted for 0.6, 1.4 and 8.0 % of total abundances of OSs in WH, NJ and SH, respectively. Only a few OSs with $\mathrm{AI}>0.5$ were identified, but it could be due to the fact that this value takes into account carbon bounded S and N but not sulfate and nitrate groups (and the related oxygen atoms), underestimating the

ACPD
15, 21415–21448, 2015

aromatic ring content. Nevertheless, BS and its analogues were detected in most of the samples of the three megacities.

Figures 3 and 4 show the CH_2-Kendrick diagrams and Van Krevelen (VK) diagrams for CHOS and CHONS species in summer, respectively, with the variation in DBE being color-coded. In the CH_2-Kendrick diagram, compounds in a homologue series i.e., compounds with identical KMD_{CH_2} values, form a horizontal line. The molecular formula of the homologue series 1 and 2, i.e., those whose DBE values were equal to zero, can be written as $C_nH_{2n+2}SO_4$ and $C_nH_{2n+2}O_1SO_4$, respectively. Hence, the OS in the homologue series 2 contained one more hydroxyl group or ether group than the corresponding one in the homologue series 1. Similarly, molecular formula of the homologue series 3, 4, and 7 with DBE = 1 can be written as $C_nH_{2n}O_1SO_4$, $C_nH_{2n}O_2SO_4$, and $C_nH_{2n}O_3SO_4$, respectively; molecular formula of the homologue series 6, 9, 11, and 13 with DBE = 2 can be written as $C_{n+1}H_{2n}O_2SO_4$, $C_{n+1}H_{2n}O_3SO_4$, $C_{n+1}H_{2n}O_4SO_4$, and $C_{n+1}H_{2n}O_5SO_4$, respectively; and molecular formula of the homologue series 5, 8, 10, 12, 14, and 15 with DBE = 3 can be written as $C_{n+2}H_{2n}O_1SO_4$, $C_{n+2}H_{2n}O_2SO_4$, $C_{n+2}H_{2n}O_3SO_4$, $C_{n+2}H_{2n}O_4SO_4$, $C_{n+2}H_{2n}O_5SO_4$, and $C_{n+2}H_{2n}O_6SO_4$, respectively. The main differences among compounds with identical DBE values are the numbers of CH_2 and oxygen atoms in the molecules. More oxygen atoms and larger DBE led to more complex combinations of functional groups. For the homologue series with DBE = 2 or 3, the oxygen atoms, excluding those in the sulfate group, probably belonged to hydroxyl groups, carbonyl groups and carboxylic groups, and it is unlikely that a compound in this molecular weight range contains so many ether groups. CHOS with DBE = 4 or 5 represented 9.9, 12.2, and 9.5 % of the total CHOS species in WH, NJ, and SH, respectively.

The H/C ratios of CHOS species are plotted vs. their $(o - 3s)/c$ ratios in the VK diagram. The more oxidized species appear in the lower right of VK diagram and the more saturated species are distributed in the upper left (Wu et al., 2004; Kim et al., 2003). The homologue series 1 and 2 with DBE = 0 constitute upward lines in the VK diagram, and within the same series, the degrees of oxidation and saturation become smaller

ACPD
15, 21415–21448, 2015

when the molecular weight increases. The homologue series 3, 4, and 7 with DBE = 1 forms one horizontal line with an identical degree of saturation, i.e., H/C = 2. For these three homologue series, a larger molecular weight corresponds to a smaller degree of oxidation within the same series. Homologue series with DBE > 1 constitute downward lines, and increasing molecular weight leads to decreasing degree of oxidation and increasing degree of saturation.

In the region where KM_{CH_2} is between 350 and 750 and KMD_{CH_2} is larger than 0.38, significant differences in CHOS species existed among three megacities. No CHOS was observed in this region in WH, whereas up to 6.5 and 9.5 % of the total CHOS, respectively, was identified in the NJ and SH samples. The CHOS species in this region were characterized by a high molecular weight, high degrees of unsaturation and oxidation (DBE > 5 and $(o - 3s)/c > 0.5$), and a minimum amount of isomers (one isomer for 79 % of CHOS in this region), corresponding to CHOS species in the lower right region of the VK diagrams. They thus likely contain one or more aromatic rings (DBE/C > 0.67, but AI < 0.5) and come most certainly form anthropogenic precursors.

Less CHONS than CHOS species were observed in samples from the three megacities. In the CH_2-Kendrick diagram, the KMD_{CH_2} values of CHONS were generally larger than those of CHOS because the presence of the additional one or two nitrates in CHONS contributes to KMD_{CH_2}. Similarly to CHOS species, CHONS species in a homologue series, i.e., with identical KMD_{CH_2} values, form a horizontal line. Molecular formula of the homologue series 1 and 3 with DBE = 1 can be written as $C_nH_{2n+1}NO_3SO_4$ and $C_nH_{2n+1}ONO_3SO_4$, respectively; molecular formula of the homologue series 2, 4, 5, and 8 with DBE = 2 can be written as $C_nH_{2n-1}NO_3SO_4$, $C_nH_{2n-1}ONO_3SO_4$, $C_nH_{2n-1}O_2NO_3SO_4$, and $C_nH_{2n-1}O_3NO_3SO_4$, respectively; molecular formula of the homologue series 7, 9, and 10 with DBE = 3 can be written as $C_{n+1}H_{2n-1}O_2NO_3SO_4$, $C_{n+1}H_{2n-1}O_3NO_3SO_4$, and $C_{n+1}H_{2n-1}O_4NO_3SO_4$, respectively; and molecular formula of the homologue series 6 with DBE = 4 can be written as $C_{n+2}H_{2n-1}ONO_3SO_4$. The main difference among CHONS species in the same homologue series is the number of CH_2, and the difference among CHONS species with an identical DBE value but not

ACPD
15, 21415–21448, 2015

in the same homologue series is the number of oxygen atoms in the formula, which is similar to the distribution of CHOS species. By comparing the molecular formula of CHOS and CHONS species, it is evident that most of CHONS could be formed by substituting one hydrogen atom in CHOS with a nitrate group.

Many differences exist between the VK diagrams of CHOS and CHONS, because x axis corresponds to the $(o-3s-2n)/c$ ratio in the VK diagram of CHONS, and CHONS contained one or two nitrate groups. The homologue series 1 and 3 constitute upward lines, and within the same series, the degrees of oxidation and saturation become smaller when the molecular weight increases. Other homologues series of CHONS form downward lines, and increasing molecular weight leads to increasing degree of saturation and decreasing degree of oxidation. CHONS species in the region where KM_{CH_2} is between 500 and 700 and KMD_{CH_2} is larger than 0.6, whose DBE values were larger than 5 with a high molecular weight and a high degree of oxidation ($(o-3s-2n)/c > 0.5$) were identified in NJ and SH. Their elemental ratios were different from any CHOS species with the same carbon number, indicating that different precursors led to their formation. On the other hand, a few additional CHONS species whose DBE values were also larger than 5 with relatively a low molecular weight and low degrees of saturation and oxidation ($(o-3s-2n)/c < 0.3$) were present in three megacities.

Figure S2 shows the numbers of CHOS and CHONS species in different mass ranges. Generally, OSs in the mass range of 250–300 Da showed the greatest variety. The number of OSs in the mass range of 200–400 Da accounted for 90.5, 83.1, and 85.4 % of identified OSs in WH, NJ and SH, respectively. OSs with molecular weight larger than 500 Da, characterized by high degrees of unsaturation as shown in the KMD diagrams, existed in the NJ and SH samples, whereas molecular weight of all OSs in the WH sample was less than 500 Da.

In summary, the characteristics of identified OSs between in NJ and in SH shared better similarity, probably because NJ and SH are geographically closer at the lower reach of the Yangtze River, whereas WH is at the middle reach of the Yangtze River.

ACPD
15, 21415–21448, 2015

It is likely that identities and levels of precursors of OSs vary a lot between the middle and lower reaches of the Yangtze River.

3.3 Formation pathways of isoprene-derived OSs in three megacities

Isoprene has been shown to be an important precursor of OSs in the three megacities. Previous studies suggest that IEPOX ($C_5H_{10}O_3$) and MAE ($C_4H_6O_3$) are two key reactive intermediates that are formed during isoprene oxidation under low- and high-NO_x conditions, respectively. Subsequent acid catalyzed-reactions of IEPOX and MAE in the presence of sulfates lead to the formation of $C_5H_{12}O_3SO_4$ and $C_4H_8O_3SO_4$, respectively (Surratt et al., 2010; Worton et al., 2013), the C_4-OS being logically promoted under high-NO_x conditions compared to the C_5 one. In this study, S/C ratio has been limited to 0–0.2 to assure that the obtained compound exists in nature (Lin et al., 2012a; Tao et al., 2014; Wozniak et al., 2008). As a result, $C_4H_8O_3SO_4$ has been eliminated by this criterion. Here we manually extract the arbitrary abundance of $C_4H_8O_3SO_4$, and compare it to that of $C_5H_{12}O_3SO_4$ to elucidate the formation pathway of isoprene-derived OSs in three megacities.

In SH, the abundance of $C_4H_8O_3SO_4$ was 8.9 times higher than that of $C_5H_{12}O_3SO_4$ during daytime in winter, whereas the abundance of $C_5H_{12}O_3SO_4$ was 4.9 times higher than that of $C_4H_8O_3SO_4$ during daytime in summer. This is clearly consistent with the assumption that the high concentration of NO_x in winter had an impact on the reaction pathway (Dong et al., 2013). In WH, the abundance of $C_5H_{12}O_3SO_4$ was 7.5 times and 4.5 times higher than that of $C_4H_8O_3SO_4$ in summer and winter in WH, respectively, also consistent with the fact that higher NO_x level in winter corresponds to more $C_4H_8O_3SO_4$, relatively. The difference between seasons is nevertheless less significant in WH than in SH. In the NJ summer daytime sample, the abundance of $C_4H_8O_3SO_4$ was greater than that of $C_5H_{12}O_3SO_4$ with ratio of about 2.5, suggesting that high NO_x pathway might dominate in summer in NJ (Dong et al., 2013).

ACPD
15, 21415–21448, 2015

3.4 Seasonal and diurnal variations of OSs in SH

During our sampling days, the air quality and meteorological conditions were similar to the general average seasonal conditions in the same year (Table S2). Therefore, the characteristics of seasonal and diurnal variations of OSs in Shanghai could be obtained through analyzing and comparing the four samples.

Contrary to the samples of the three cities, all the SH samples were collected and analyzed under the same conditions (sampling time of 12 h for daytime and nighttime, same injection volume for LC-MS analysis). For more accurate comparison purpose, it was chosen in this section to arbitrary set the abundance of $C_{10}H_{17}NO_3SO_4$ in the nighttime summer sample (the highest one from all the SH samples) to 100 % and to define a limit corresponding 0.5 % of this value. This absolute abundance limit value was applied to all the four SH samples to include or not the OSs of in the data presented here. Even if the data are not quantitative, defining such a limiting abundance for samples collected and analyzed under same conditions is equivalent to define a unique minimal concentration below which the OSs are not taken into account and disconnects the selection rule from the abundance of the major compound in each sample. Note that less OSs are consequently discussed in this section than in the previous ones.

Figure 5 shows that the number of OSs in summer was much larger than that in winter, and that the number of OSs, especially the number of CHONS, at night was much larger than that in the daytime. As shown in Fig. 6, the total arbitrary abundances of OSs in the summer daytime and nighttime samples were 2.1 times and 3.0 times of that in the corresponding winter samples, respectively. The total arbitrary abundances of OSs in the summer and winter nighttime samples were 1.8 times and 1.3 times of that in the corresponding daytime samples, respectively. In addition, the arbitrary abundances of CHOS did not show a clear diurnal variation, whereas the arbitrary abundances of CHONS in the summer and winter nighttime samples were 5.0 times and 2.2 times of that in the corresponding daytime samples, respectively. This is consistent

ACPD
15, 21415–21448, 2015

with the previous observation from Fig. 2 (see Sect. 3.1) that CHONS are much more present during nighttime. The variety (Fig. 5) and the abundance (Fig. 6) of CHONS at night were both far larger than those during daytime, in winter and in summer. Besides, CHONS abundance is larger in summer than in winter. CHONS formation seems thus both driven by daytime photochemistry and subsequent nighttime NO_3 chemistry. Similar observations were done in Beijing, China (van Pinxteren et al., 2009), Atlanta, GA (Hatch et al., 2011) and Bakersfield, CA, USA (O'Brien et al., 2014). However, He et al. (2014) observed a reverse trend at a regional background site in the Pearl River Delta region (higher concentrations of nitrooxy-OSs existed during daytime), concluding that photochemical reactions could also lead to the formation of significant amount nitrooxy-OSs. These pathways could contribute here to the daytime low abundance of CHONS.

Figure 6 further exhibits the carbon number-based arbitrary abundance of CHOS and CHONS. In all the four samples, more than 60 % of OSs were characterized by 5 to 10 carbon atoms, i.e., C_5–C_{10}, in their carbon chain moiety. In summer samples, C_5 and C_{10} were the most abundant, suggesting that isoprene and monoterpenes could be the main precursors. In winter, in addition to C_5 and C_{10}, the relative abundances of C_8, C_9, and C_{14+} were also high, hinting additional precursors. In contrast, C_{10} that were derived from monoterpenes always represented the dominant category in spring, autumn, and winter in the Pearl River Delta, South China, and in Taiwan (Lin et al., 2012b), maybe underlying a lesser anthropogenic influence in these two regions than in the Yangtze River region.

The VK diagrams of CHOS and CHONS in the SH samples are presented in Fig. S3, which represents a combination of Figs. 3 and 4 (with a lesser number of OSs accounted for). OSs in the four samples were characterized by similar degrees of saturation. OSs with a low degree of saturation and a high molecular weight existed in all four samples. From Table 1 and Fig. S3, it can be concluded that the average degree of oxidation of OSs in summer was higher than that in winter, because many highly oxidized OSs existed in summer samples.

ACPD
15, 21415–21448, 2015

4 Conclusions

In this study, atmospheric $PM_{2.5}$ samples in WH, NJ, and SH were analyzed using an UHPLC-Orbitrap MS. Aliphatic OSs represented at least 78 % of the identified OSs at three locations, and aromatic OSs were much less. In addition, the number of isomers of OSs varied in the three megacities. In WH, the number of OSs with six and more isomers accounted for the highest percentage while OSs with only one isomer were present in a small amount. On the contrary, the percentage of OSs with six and more isomers was pretty low, and the percentage of OSs with one isomer was pretty large in NJ and SH. Besides, the average molecular weight and degree of saturation of OSs in NJ and SH were similar, whereas the average degree of oxidation of OSs in NJ was slightly smaller than that in SH. On the other hand, in summer, the average molecular weight and degree of oxidation of OSs in WH were the lowest among three megacities, but the average degree of saturation was the highest. Therefore, it can be concluded that the aerosol samples from NJ and SH shared more similarities. Although isoprene was most likely one of the important precursors in the three megacities, the reaction pathways leading to isoprene-derived OSs probably varied because of the impact of NO_x levels.

In SH, the relative abundance of OSs in summer was far greater than those in winter. While no clear diurnal variation was observed for CHOS, more nitrooxy-OSs existed at night, probably because of active NO_3 radical chemistry at night. In SH samples, C_5 and C_{10} were the most abundant in summer, indicating the importance of isoprene and monoterpenes as precursors of OSs, whereas C_8, C_9, and C_{14+} were also abundant in winter, hinting other potential precursors in winter.

The general characteristics including the average molecular weight, degrees of oxidation and saturation, and the number of isomers of OSs in the atmospheric $PM_{2.5}$ in three megacities, and the seasonal and diurnal variations of OSs in SH were presented in this study. Clearly, precursors and formation mechanisms of many OSs are yet to be

ACPD
15, 21415–21448, 2015

elucidated, which demands further studies with better identification and quantification methods.

The Supplement related to this article is available online at doi:10.5194/acpd-15-21415-2015-supplement.

Acknowledgements. This study was financially supported by the National Natural Science Foundation of China (No. 21 107 015, 21 190 053, and 21 222 703), the Special Fund for Ph.D. Studies from Ministry of Education of China (20 120 071 110 023), and the Cyrus Tang Foundation (No. CTF-FD2 014 001). LW thanks the Newton Advanced Fellowship (NA140 106). CG thanks the support by the European Research Council under the European Union's Seventh Framework Programme (FP/2007–2013)/ERC Grant Agreement 290 852 – AIRSEA, and the Marie Curie International Research Staff Exchange project AMIS (Grant 295 132).

References

Andreae, M. O. and Crutzen, P. J.: Atmospheric aerosols: biogeochemical sources and role in atmospheric chemistry, Science, 276, 1052–1058, doi:10.1126/science.276.5315.1052, 1997.

Chan, M. N., Surratt, J. D., Chan, A. W. H., Schilling, K., Offenberg, J. H., Lewandowski, M., Edney, E. O., Kleindienst, T. E., Jaoui, M., Edgerton, E. S., Tanner, R. L., Shaw, S. L., Zheng, M., Knipping, E. M., and Seinfeld, J. H.: Influence of aerosol acidity on the chemical composition of secondary organic aerosol from β-caryophyllene, Atmos. Chem. Phys., 11, 1735–1751, doi:10.5194/acp-11-1735-2011, 2011.

Darer, A. I., Cole-Filipiak, N. C., O'Connor, A. E., and Elrod, M. J.: Formation and stability of atmospherically relevant isoprene-derived organosulfates and organonitrates, Environ. Sci. Technol., 45, 1895–1902, doi:10.1021/es103797z, 2011.

Dong, X. Y., Gao, Y., Fu, J. S., Li, J., Huang, K., Zhuang, G. S., and Zhou, Y.: Probe into gaseous pollution and assessment of air quality benefit under sector dependent emission control strategies over megacities in Yangtze River Delta, China, Atmos. Environ., 79, 841–852, doi:10.1016/j.atmosenv.2013.07.041, 2013.

ACPD
15, 21415–21448, 2015

Fuller, S. J., Zhao, Y. J., Cliff, S. S., Wexler, A. S., and Kalberer, M.: Direct surface analysis of time-resolved aerosol impactor samples with ultrahigh-resolution mass spectrometry, Anal. Chem., 84, 9858–9864, doi:10.1021/ac3020615, 2012.

Gomez-Gonzalez, Y., Surratt, J. D., Cuyckens, F., Szmigielski, R., Vermeylen, R., Jaoui, M., Lewandowski, M., Offenberg, J. H., Kleindienst, T. E., Edney, E. O., Blockhuys, F., Van Alsenoy, C., Maenhaut, W., and Claeys, M.: Characterization of organosulfates from the photooxidation of isoprene and unsaturated fatty acids in ambient aerosol using liquid chromatography/(-) electrospray ionization mass spectrometry, J. Mass Spectrom., 43, 371–382, doi:10.1002/jms.1329, 2008.

Guenther, A., Hewitt, C. N., Erickson, D., Fall, R., Geron, C., Graedel, T., Harley, P., Klinger, L., Lerdau, M., McKay, W. A., Pierce, T., Scholes, B., Steinbrecher, R., Tallamraju, R., Taylor, J., and Zimmerman, P.: A global-model of natural volatile organic-compound emissions, J. Geophys. Res.-Atmos., 100, 8873–8892, doi:10.1029/94jd02950, 1995.

Hallquist, M., Wenger, J. C., Baltensperger, U., Rudich, Y., Simpson, D., Claeys, M., Dommen, J., Donahue, N. M., George, C., Goldstein, A. H., Hamilton, J. F., Herrmann, H., Hoffmann, T., Iinuma, Y., Jang, M., Jenkin, M. E., Jimenez, J. L., Kiendler-Scharr, A., Maenhaut, W., McFiggans, G., Mentel, Th. F., Monod, A., Prévôt, A. S. H., Seinfeld, J. H., Surratt, J. D., Szmigielski, R., and Wildt, J.: The formation, properties and impact of secondary organic aerosol: current and emerging issues, Atmos. Chem. Phys., 9, 5155–5236, doi:10.5194/acp-9-5155-2009, 2009.

Hatch, L. E., Creamean, J. M., Ault, A. P., Surratt, J. D., Chan, M. N., Seinfeld, J. H., Edgerton, E. S., Su, Y. X., and Prather, K. A.: Measurements of isoprene-derived organosulfates in ambient aerosols by aerosol time-of-flight mass spectrometry – Part 2: Temporal variability and formation mechanisms, Environ. Sci. Technol., 45, 8648–8655, doi:10.1021/es2011836, 2011.

Hawkins, L. N., Russell, L. M., Covert, D. S., Quinn, P. K., and Bates, T. S.: Carboxylic acids, sulfates, and organosulfates in processed continental organic aerosol over the southeast Pacific Ocean during VOCALS-REx 2008, J. Geophys. Res.-Atmos., 115, D13201, doi:10.1029/2009jd013276, 2010.

He, Q. F., Ding, X., Wang, X. M., Yu, J. Z., Fu, X. X., Liu, T. Y., Zhang, Z., Xue, J., Chen, D. H., Zhong, L. J., and Donahue, N. M.: Organosulfates from pinene and isoprene over the Pearl River Delta, south China: seasonal variation and implication in formation mechanisms, Environ. Sci. Technol., 48, 9236–9245, doi:10.1021/es501299v, 2014.

ACPD
15, 21415–21448, 2015

Hu, K. S., Darer, A. I., and Elrod, M. J.: Thermodynamics and kinetics of the hydrolysis of atmospherically relevant organonitrates and organosulfates, Atmos. Chem. Phys., 11, 8307–8320, doi:10.5194/acp-11-8307-2011, 2011.

Huang, C., Chen, C. H., Li, L., Cheng, Z., Wang, H. L., Huang, H. Y., Streets, D. G., Wang, Y. J., Zhang, G. F., and Chen, Y. R.: Emission inventory of anthropogenic air pollutants and VOC species in the Yangtze River Delta region, China, Atmos. Chem. Phys., 11, 4105–4120, doi:10.5194/acp-11-4105-2011, 2011.

Iinuma, Y., Muller, C., Berndt, T., Boge, O., Claeys, M., and Herrmann, H.: Evidence for the existence of organosulfates from beta-pinene ozonolysis in ambient secondary organic aerosol, Environ. Sci. Technol., 41, 6678–6683, doi:10.1021/es070938t, 2007a.

Iinuma, Y., Muller, C., Boge, O., Gnauk, T., and Herrmann, H.: The formation of organic sulfate esters in the limonene ozonolysis secondary organic aerosol (SOA) under acidic conditions, Atmos. Environ., 41, 5571–5583, doi:10.1016/j.atmosenv.2007.03.007, 2007b.

Kim, S., Kramer, R. W., and Hatcher, P. G.: Graphical method for analysis of ultrahigh-resolution broadband mass spectra of natural organic matter, the van Krevelen diagram, Anal. Chem., 75, 5336–5344, doi:10.1021/ac034415p, 2003.

Koch, B. P. and Dittmar, T.: From mass to structure: an aromaticity index for high-resolution mass data of natural organic matter, Rapid Commun. Mass Sp., 20, 926–932, doi:10.1002/rcm.2386, 2006.

Kristensen, K. and Glasius, M.: Organosulfates and oxidation products from biogenic hydrocarbons in fine aerosols from a forest in North West Europe during spring, Atmos. Environ., 45, 4546–4556, doi:10.1016/j.atmosenv.2011.05.063, 2011.

Kundu, S., Quraishi, T. A., Yu, G., Suarez, C., Keutsch, F. N., and Stone, E. A.: Evidence and quantitation of aromatic organosulfates in ambient aerosols in Lahore, Pakistan, Atmos. Chem. Phys., 13, 4865–4875, doi:10.5194/acp-13-4865-2013, 2013.

Lee, P. K., Youm, S. J., and Jo, H. Y.: Heavy metal concentrations and contamination levels from Asian dust and identification of sources: a case-study, Chemosphere, 91, 1018–1025, doi:10.1016/j.chemosphere.2013.01.074, 2013.

Liggio, J., Li, S. M., and McLaren, R.: Heterogeneous reactions of glyoxal on particulate matter: identification of acetals and sulfate esters, Environ. Sci. Technol., 39, 1532–1541, doi:10.1021/es048375y, 2005.

Lin, P., Rincon, A. G., Kalberer, M., and Yu, J. Z.: Elemental composition of HULIS in the Pearl River Delta region, China: results inferred from positive and negative electro-

ACPD
15, 21415–21448, 2015

spray high resolution mass spectrometric data, Environ. Sci. Technol., 46, 7454–7462, doi:10.1021/es300285d, 2012a.
Lin, P., Yu, J. Z., Engling, G., and Kalberer, M.: Organosulfates in humic-like substance fraction isolated from aerosols at seven locations in East Asia: a study by ultra-high-resolution mass spectrometry, Environ. Sci. Technol., 46, 13118–13127, doi:10.1021/es303570v, 2012b.
Ma, Y., Chen, J. M., and Wang, L.: Characteristics and formation mechanisms of atmospheric organosulfates, Prog. Chem., 24, 2277–2286, 2012.
Ma, Y., Xu, X. K., Song, W. H., Geng, F. H., and Wang, L.: Seasonal and diurnal variations of particulate organosulfates in urban Shanghai, China, Atmos. Environ., 85, 152–160, doi:10.1016/j.atmosenv.2013.12.017, 2014.
O'Brien, R. E., Laskin, A., Laskin, J., Rubitschun, C. L., Surratt, J. D., and Goldstein, A. H.: Molecular characterization of S- and N-containing organic constituents in ambient aerosols by negative ion mode high-resolution nanospray desorption electrospray ionization mass spectrometry: CalNex 2010 field study, J. Geophys. Res.-Atmos., 119, 12706–12720, doi:10.1002/2014jd021955, 2014.
Olson, C. N., Galloway, M. M., Yu, G., Hedman, C. J., Lockett, M. R., Yoon, T., Stone, E. A., Smith, L. M., and Keutsch, F. N.: Hydroxycarboxylic acid-derived organosulfates: synthesis, stability, and quantification in ambient aerosol, Environ. Sci. Technol., 45, 6468–6474, doi:10.1021/es201039p, 2011.
Paulot, F., Crounse, J. D., Kjaergaard, H. G., Kurten, A., St Clair, J. M., Seinfeld, J. H., and Wennberg, P. O.: Unexpected epoxide formation in the gas-phase photooxidation of isoprene, Science, 325, 730–733, doi:10.1126/science.1172910, 2009.
Staudt, S., Kundu, S., Lehmler, H. J., He, X. R., Cui, T. Q., Lin, Y. H., Kristensen, K., Glasius, M., Zhang, X. L., Weber, R. J., Surratt, J. D., and Stone, E. A.: Aromatic organosulfates in atmospheric aerosols: synthesis, characterization, and abundance, Atmos. Environ., 94, 366–373, doi:10.1016/j.atmosenv.2014.05.049, 2014.
Stone, E. A., Hedman, C. J., Sheesley, R. J., Shafer, M. M., and Schauer, J. J.: Investigating the chemical nature of humic-like substances (HULIS) in North American atmospheric aerosols by liquid chromatography tandem mass spectrometry, Atmos. Environ., 43, 4205–4213, doi:10.1016/j.atmosenv.2009.05.030, 2009.
Surratt, J. D., Kroll, J. H., Kleindienst, T. E., Edney, E. O., Claeys, M., Sorooshian, A., Ng, N. L., Offenberg, J. H., Lewandowski, M., Jaoui, M., Flagan, R. C., and Seinfeld, J. H.: Evi-

ACPD
15, 21415–21448, 2015

dence for organosulfates in secondary organic aerosol, Environ. Sci. Technol., 41, 517–527, doi:10.1021/es062081q, 2007.
Surratt, J. D., Gomez-Gonzalez, Y., Chan, A. W. H., Vermeylen, R., Shahgholi, M., Kleindienst, T. E., Edney, E. O., Offenberg, J. H., Lewandowski, M., Jaoui, M., Maenhaut, W., Claeys, M., Flagan, R. C., and Seinfeld, J. H.: Organosulfate formation in biogenic secondary organic aerosol, J. Phys. Chem. A, 112, 8345–8378, doi:10.1021/jp802310p, 2008.
Surratt, J. D., Chan, A. W. H., Eddingsaas, N. C., Chan, M. N., Loza, C. L., Kwan, A. J., Hersey, S. P., Flagan, R. C., Wennberg, P. O., and Seinfeld, J. H.: Reactive intermediates revealed in secondary organic aerosol formation from isoprene, P. Natl. Acad. Sci. USA, 107, 6640–6645, doi:10.1073/pnas.0911114107, 2010.
Tao, S., Lu, X., Levac, N., Bateman, A. P., Nguyen, T. B., Bones, D. L., Nizkorodov, S. A., Laskin, J., Laskin, A., and Yang, X.: Molecular characterization of organosulfates in organic aerosols from Shanghai and Los Angeles urban areas by nanospray-desorption electrospray ionization high-resolution mass spectrometry, Environ. Sci. Technol., 48, 10993–11001, doi:10.1021/es5024674, 2014.
Tolocka, M. P. and Turpin, B.: Contribution of organosulfur compounds to organic aerosol mass, Environ. Sci. Technol., 46, 7978–7983, doi:10.1021/es300651v, 2012.
van Pinxteren, D., Bruggemann, E., Gnauk, T., Iinuma, Y., Muller, K., Nowak, A., Achtert, P., Wiedensohler, A., and Herrmann, H.: Size- and time-resolved chemical particle characterization during CAREBeijing-2006: different pollution regimes and diurnal profiles, J. Geophys. Res.-Atmos., 114, D00g09, doi:10.1029/2008jd010890, 2009.
Wang, L., Du, H. H., Chen, J. M., Zhang, M., Huang, X. Y., Tan, H. B., Kong, L. D., and Geng, F. H.: Consecutive transport of anthropogenic air masses and dust storm plume: two case events at Shanghai, China, Atmos. Res., 127, 22–33, doi:10.1016/j.atmosres.2013.02.011, 2013.
Worton, D. R., Surratt, J. D., LaFranchi, B. W., Chan, A. W. H., Zhao, Y. L., Weber, R. J., Park, J. H., Gilman, J. B., de Gouw, J., Park, C., Schade, G., Beaver, M., St Clair, J. M., Crounse, J., Wennberg, P., Wolfe, G. M., Harrold, S., Thornton, J. A., Farmer, D. K., Docherty, K. S., Cubison, M. J., Jimenez, J. L., Frossard, A. A., Russell, L. M., Kristensen, K., Glasius, M., Mao, J. Q., Ren, X. R., Brune, W., Browne, E. C., Pusede, S. E., Cohen, R. C., Seinfeld, J. H., and Goldsteint, A. H.: Observational insights into aerosol formation from isoprene, Environ. Sci. Technol., 47, 11403–11413, doi:10.1021/es4011064, 2013.

ACPD
15, 21415–21448, 2015

Wozniak, A. S., Bauer, J. E., Sleighter, R. L., Dickhut, R. M., and Hatcher, P. G.: Technical Note: Molecular characterization of aerosol-derived water soluble organic carbon using ultrahigh resolution electrospray ionization Fourier transform ion cyclotron resonance mass spectrometry, Atmos. Chem. Phys., 8, 5099–5111, doi:10.5194/acp-8-5099-2008, 2008.

Wu, Z. G., Rodgers, R. P., and Marshall, A. G.: Two- and three-dimensional van Krevelen diagrams: a graphical analysis complementary to the Kendrick mass plot for sorting elemental compositions of complex organic mixtures based on ultrahigh-resolution broadband Fourier transform ion cyclotron resonance mass measurements, Anal. Chem., 76, 2511–2516, doi:10.1021/ac0355449, 2004.

Xiao, S., Wang, M. Y., Yao, L., Kulmala, M., Zhou, B., Yang, X., Chen, J. M., Wang, D. F., Fu, Q. Y., Worsnop, D. R., and Wang, L.: Strong atmospheric new particle formation in winter in urban Shanghai, China, Atmos. Chem. Phys., 15, 1769–1781, doi:10.5194/acp-15-1769-2015, 2015.

Zhang, H. F., Worton, D. R., Lewandowski, M., Ortega, J., Rubitschun, C. L., Park, J. H., Kristensen, K., Campuzano-Jost, P., Day, D. A., Jimenez, J. L., Jaoui, M., Offenberg, J. H., Kleindienst, T. E., Gilman, J., Kuster, W. C., de Gouw, J., Park, C., Schade, G. W., Frossard, A. A., Russell, L., Kaser, L., Jud, W., Hansel, A., Cappellin, L., Karl, T., Glasius, M., Guenther, A., Goldstein, A. H., Seinfeld, J. H., Gold, A., Kamens, R. M., and Surratt, J. D.: Organosulfates as tracers for secondary organic aerosol (SOA) formation from 2-Methyl-3-Buten-2-ol (MBO) in the atmosphere, Environ. Sci. Technol., 46, 9437–9446, doi:10.1021/es301648z, 2012.

Zheng, J., Ma, Y., Chen, M. D., Zhang, Q., Wang, L., Khalizov, A. F., Yao, L., Wang, Z., Wang, X., and Chen, L. X.: Measurement of atmospheric amines and ammonia using the high resolution time-of-flight chemical ionization mass spectrometry, Atmos. Environ., 102, 249–259, doi:10.1016/j.atmosenv.2014.12.002, 2015.

ACPD
15, 21415–21448, 2015

Table 1. Summary of sampling location, sampling time, and Molecular Weight (MW), Double Bond Equivalents (DBE), and Elemental Ratios (arithmetic mean ± standard deviation) of identified CHOS and CHONS.

Sample ID	location	sampling time	number of formulas CHOS/CHONS	CHOS[a] MW	CHOS DBE	CHOS $(o-3s)/c$[c]	CHOS H/C[d]	CHONS[b] MW	CHONS DBE	CHONS $(o-3s-2n)/c$[e]	CHONS H/C
WH	Wuhan	9:00 a.m., 26 Jan–9:00 a.m., 27 Jan 2012	149/43	266.6 ± 57.2	2.56 ± 2.60	0.37 ± 0.25	1.68 ± 0.44	311.0 ± 60.5	3.61 ± 2.57	0.35 ± 0.13	1.58 ± 0.46
		8:30 a.m., 15 Jun–8:30 a.m., 16 Jun 2012	213/55	287.9 ± 60.8	2.16 ± 1.64	0.39 ± 0.23	1.75 ± 0.36	318.1 ± 53.8	2.98 ± 1.52	0.40 ± 0.17	1.69 ± 0.34
NJ	Nanjing	7:30 a.m.–7:30 p.m., 29 Aug 2012	139/54	288.9 ± 67.9	1.82 ± 1.32	0.39 ± 0.25	1.83 ± 0.27	313.6 ± 48.2	2.56 ± 1.08	0.44 ± 0.21	1.79 ± 0.23
		7:30 p.m., 29 Aug–7:30 a.m., 30 Aug 2012	160/72	294.0 ± 97.3	3.21 ± 3.84	0.46 ± 0.34	1.65 ± 0.45	335.2 ± 74.3	3.46 ± 2.30	0.43 ± 0.20	1.66 ± 0.37
		combination[f]	205/83	304.8 ± 93.5	3.00 ± 3.47	0.43 ± 0.32	1.68 ± 0.41	332.5 ± 70.7	3.28 ± 2.21	0.44 ± 0.21	1.69 ± 0.35
SH	Shanghai	7:30 a.m.–7:30 p.m., 17 Jan 2013	125/32	274.3 ± 81.1	2.38 ± 2.56	0.39 ± 0.31	1.72 ± 0.46	328.7 ± 132.2	4.22 ± 3.95	0.44 ± 0.33	1.53 ± 0.57
		7:30 p.m., 17 Jan–7:30 a.m., 18 Jan 2013	159/54	270.0 ± 71.1	2.54 ± 2.39	0.40 ± 0.29	1.69 ± 0.44	303.9 ± 51.9	2.98 ± 2.50	0.38 ± 0.17	1.71 ± 0.46
		combination[f]	168/59	277.2 ± 71.2	2.63 ± 2.59	0.40 ± 0.29	1.68 ± 0.46	325.8 ± 92.0	3.59 ± 3.50	0.42 ± 0.27	1.64 ± 0.52
		8:00 a.m.–8:00 p.m., 28 Jul 2013	165/40	296.4 ± 84.7	2.76 ± 2.66	0.47 ± 0.32	1.68 ± 0.42	348.2 ± 115.4	4.03 ± 3.48	0.61 ± 0.43	1.55 ± 0.52
		8:00 p.m., 28 Jul–8:00 a.m., 29 Jul 2013	122/51	278.1 ± 73.9	2.36 ± 2.48	0.48 ± 0.29	1.74 ± 0.40	319.2 ± 73.0	3.26 ± 2.93	0.45 ± 0.22	1.69 ± 0.44
		combination[f]	168/58	296.3 ± 84.7	2.77 ± 2.65	0.47 ± 0.31	1.68 ± 0.42	337.6 ± 102.2	3.52 ± 3.04	0.53 ± 0.38	1.64 ± 0.47

[a] Molecules with $(o-4s)/c < 0$ were not included.
[b] Molecules with $(o-4s-3n)/c < 0$ were not included.
[c] $(o-3s)/c$ infers to the extent of oxidation for a CHOS molecule.
[d] H/C refers to the ratio between hydrogen atom and carbon atom in a molecule.
[e] $(o-3s-2n)/c$ refers to the extent of oxidation for a CHONS molecule.
[f] Combination of two samples for a comparison purpose.

ACPD
15, 21415–21448, 2015

Figure 1. Locations of Wuhan (WH), Nanjing (NJ), and Shanghai (SH) in China.

ACPD
15, 21415–21448, 2015

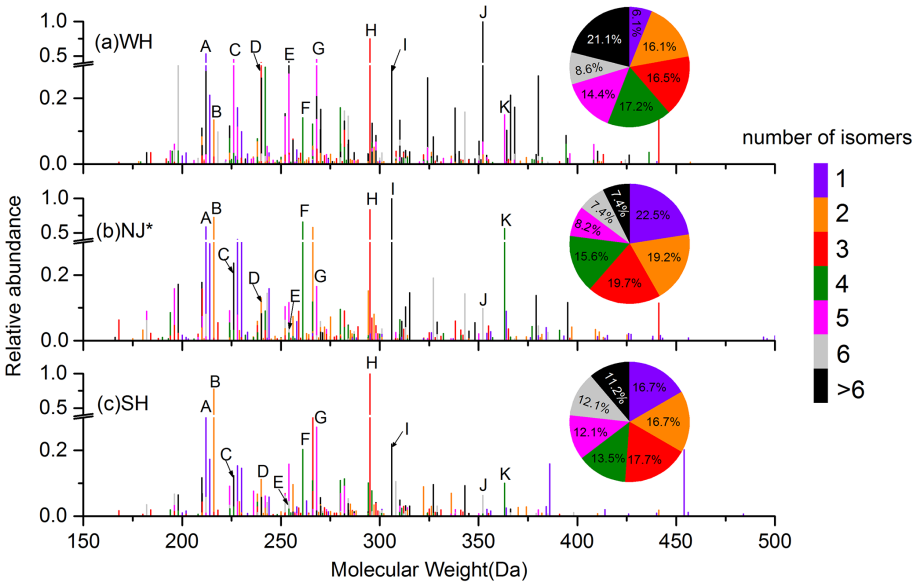

Figure 2. Mass spectra of detected CHOS and CHONS reconstructed from ion extracted chromatograms (UHPLC-Orbitrap MS analysis, negative ionization mode). *X* axis corresponds to the molecular weight (Da) of identified species. The number of isomers for a given species is marked by colors. A, neutral mass = 211.9993 Da, $C_5H_8O_7S_1$; B, neutral mass = 216.0306 Da, $C_5H_{12}O_7S_1$; C, neutral mass = 226.0150 Da, $C_6H_{10}O_7S_1$; D, neutral mass = 240.0307 Da, $C_7H_{12}O_7S_1$; E, neutral mass = 254.0827 Da, $C_9H_{18}O_6S_1$; F, neutral mass = 261.0157 Da, $C_5H_{11}O_9N_1S_1$; G, neutral mass = 268.0620 Da, $C_9H_{16}O_7S_1$; H, neutral mass = 295.0729 Da, $C_{10}H_{17}O_7N_1S_1$; I, neutral mass = 306.0007 Da, $C_5H_{10}O_{11}N_2S_1$; J, neutral mass = 352.1922 Da, $C_{16}H_{32}O_6S_1$; K, neutral mass = 363.1356, Da $C_{15}H_{25}O_7N_1S_1$. WH corresponds to the daily sample collected from 8:30 a.m., 15 June to 8:30 a.m., 16 June 2012; NJ corresponds to the nighttime sample collected from 7:30 p.m., 29 August to 7:30 a.m., 30 August 2012; SH corresponds to the daily data, i.e., to the combination of samples collected from 8:00 a.m. to 8:00 p.m., 28 July 2013 and from 8:00 p.m., 28 July to 8:00 a.m., 29 July 2013.

ACPD
15, 21415–21448, 2015

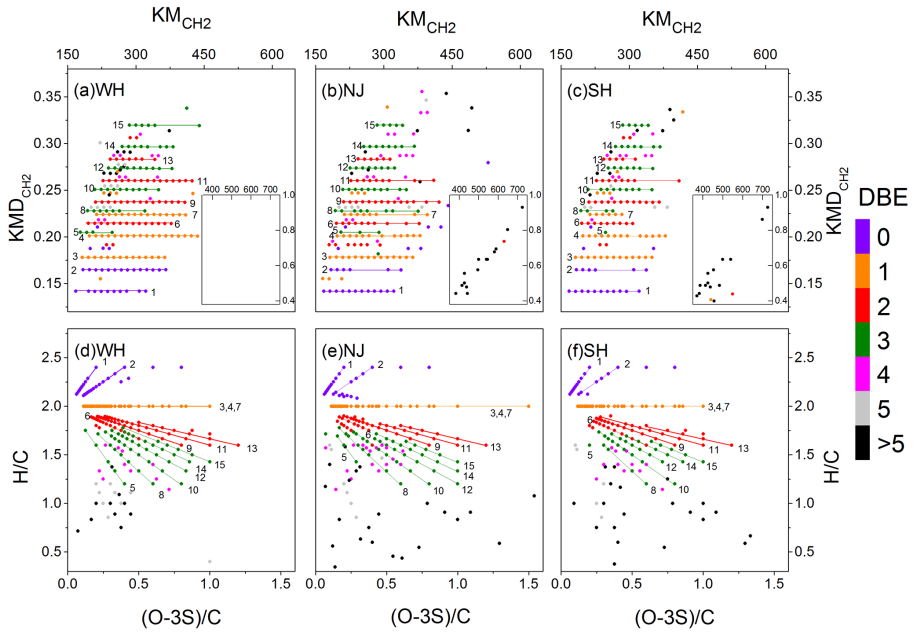

Figure 3. (a–c) CH_2-Kendrick diagrams and **(d–e)** Van Krevelen diagrams for CHOS detected in WH, NJ and SH samples. The color-coding indicates the DBE values calculated from Eq. (1). WH corresponds to the daily sample collected from 8:30 a.m., 15 June to 8:30 a.m., 16 June 2012; NJ corresponds to the daily data, i.e., to the combination of samples collected from 7:30 a.m. to 7:30 p.m., 29 August 2012 and from 7:30 p.m., 29 August to 7:30 a.m., 30 August 2012; SH corresponds to the daily data, i.e., to the combination of samples collected from 8:00 a.m. to 8:00 p.m., 28 July 2013 and from 8:00 p.m., 28 July to 8:00 a.m., 29 July 2013.

ACPD
15, 21415–21448, 2015

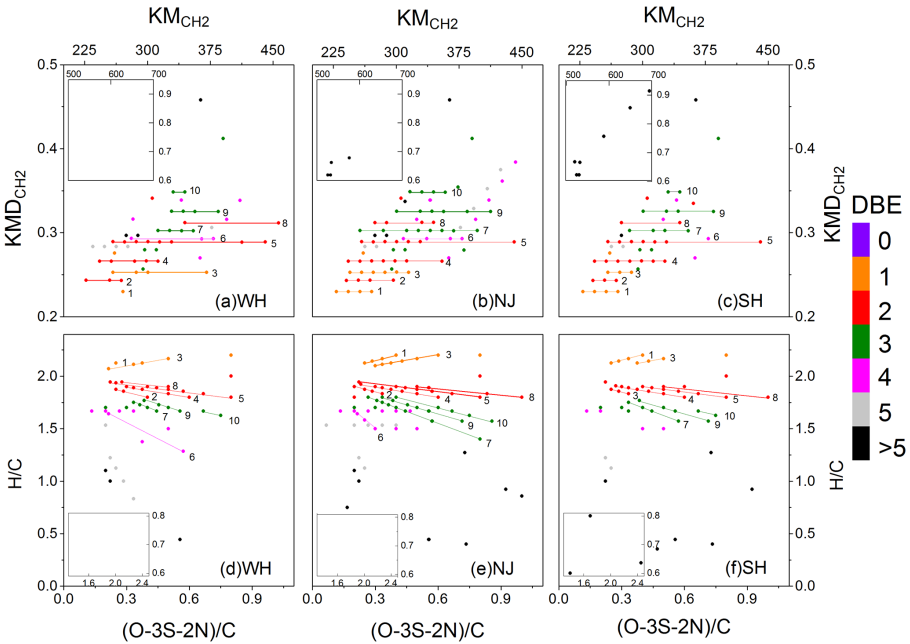

Figure 4. (a–c) CH_2-Kendrick diagrams and **(d–e)** Van Krevelen diagrams for CHONS detected in WH, NJ and SH. WH corresponds to the daily sample collected from 8:30 a.m., 15 June to 8:30 a.m., 16 June 2012; NJ corresponds to the daily data, i.e., to the combination of samples collected from 7:30 a.m. to 7:30 p.m., 29 August 2012 and from 7:30 p.m., 29 August to 7:30 a.m., 30 August 2012; SH corresponds to the daily data, i.e., to the combination of samples collected from 8:00 a.m. to 8:00 p.m., 28 July 2013 and from 8:00 p.m., 28 July to 8:00 a.m., 29 July 2013.

ACPD
15, 21415–21448, 2015

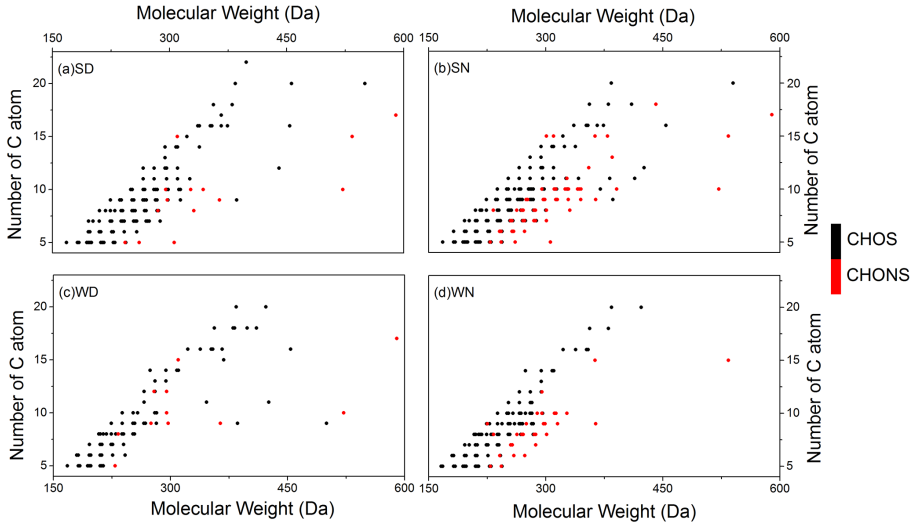

Figure 5. Number of C atoms of CHOS and CHONS as a function of molecular weight in the Shanghai samples. SD: summer day; SN: summer night; WD: winter day; WN: winter night. Note that only compounds with a relative abundance greater than or equal to 0.5 % of that of $C_{10}H_{17}O_7N_1S_1$ in the SN sample are shown in this figure.

ACPD
15, 21415–21448, 2015

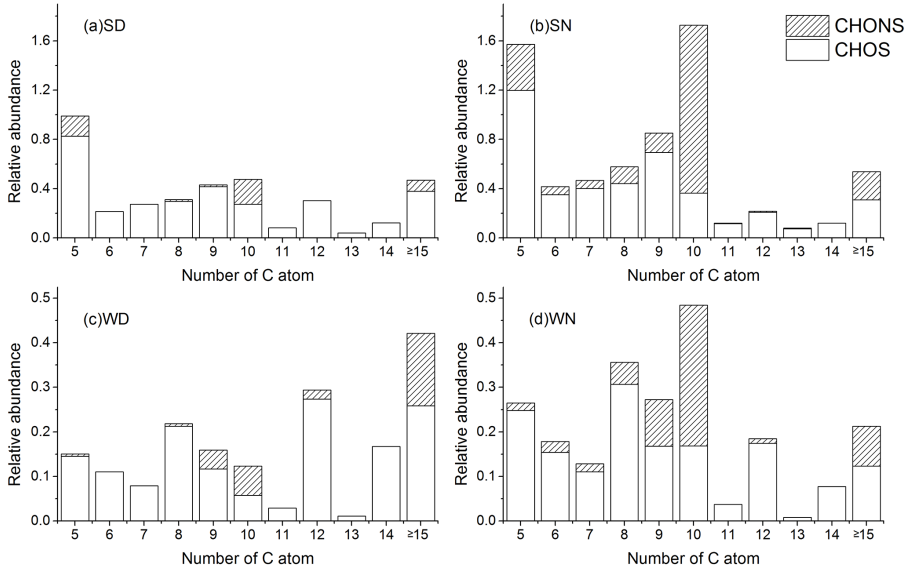

Figure 6. Relative abundance distributions of CHOS and CHONS in the Shanghai samples. SD: summer day; SN: summer night; WD: winter day; WN: winter night. Note that only compounds with a relative abundance greater than or equal to 0.5 % of that of $C_{10}H_{17}O_7N_1S_1$ in the SN sample are shown in this figure.

ACPD
15, 21415–21448, 2015